NASA TECHNICAL NOTE

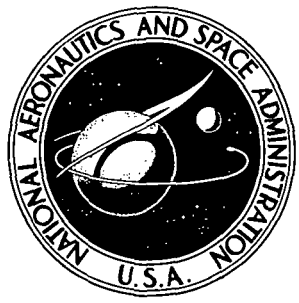

NASA TN D-7260

NASA TN D-7260

ANALYSIS OF HEAT TRANSFER FOR A NORMALLY IMPINGING LIQUID-METAL SLOT JET

by Robert Siegel

Lewis Research Center
Cleveland, Ohio 44135

NATIONAL AERONAUTICS AND SPACE ADMINISTRATION • WASHINGTON, D. C. • APRIL 1973

1. Report No.	2. Government Accession No.	3. Recipient's Catalog No.
NASA TN D-7260		

4. Title and Subtitle	5. Report Date
ANALYSIS OF HEAT TRANSFER FOR A NORMALLY IMPINGING LIQUID-METAL SLOT JET	April 1973
	6. Performing Organization Code

7. Author(s)	8. Performing Organization Report No.
Robert Siegel	E-7222
	10. Work Unit No.
	501-24

9. Performing Organization Name and Address	11. Contract or Grant No.
Lewis Research Center National Aeronautics and Space Administration Cleveland, Ohio 44135	

12. Sponsoring Agency Name and Address	13. Type of Report and Period Covered
National Aeronautics and Space Administration Washington, D.C. 20546	Technical Note
	14. Sponsoring Agency Code

15. Supplementary Notes

16. Abstract

The analysis treats a two-dimensional liquid-metal slot jet that is impinging normally against a uniformly heated flat plate. The distributions of wall temperature and heat-transfer coefficient are obtained as functions of position along the plate. The liquid-metal assumptions are made that the jet is inviscid and that molecular conduction is dominating heat diffusion. The solution is obtained by mapping the jet flow region into a potential plane where it occupies a strip of uniform width. The energy equation is transformed into potential coordinates, and an exact solution obtained in the strip region. Conformal mapping is then used to transform the solution into the physical plane.

17. Key Words (Suggested by Author(s))	18. Distribution Statement
Impingement heat transfer; Jet heat transfer; Jet impingement; Liquid-metal heat transfer; Liquid-metal jet	Unclassified - unlimited

19. Security Classif. (of this report)	20. Security Classif. (of this page)	21. No. of Pages	22. Price*
Unclassified	Unclassified	32	$3.00

* For sale by the National Technical Information Service, Springfield, Virginia 22151

ANALYSIS OF HEAT TRANSFER FOR A NORMALLY IMPINGING LIQUID-METAL SLOT JET

by Robert Siegel

Lewis Research Center

SUMMARY

Liquid metals are very effective heat-transfer fluids. For critical local cooling applications a useful technique may be to use an impinging liquid-metal jet. In this report a two-dimensional analysis is performed for a liquid-metal slot jet impinging normally against a flat plate that is heated uniformly. Wall temperatures and heat-transfer coefficients are obtained as functions of position along the plate for various values of the Peclet number. Liquid metals are low Prandtl number fluids, and as a consequence a thermal boundary layer will develop much more rapidly than a viscous layer. The fluid can then be approximated as inviscid because the viscous layer is of minor importance in the thermal-boundary-layer growth. It is also assumed that turbulence is small so that molecular conduction is dominating the diffusion of heat. The solution is obtained by mapping the jet flow region into a potential plane in which the region occupies a strip of uniform width. The energy equation is transformed into potential coordinates, and an exact solution is obtained in the strip region. Conformal mapping is then used to transform the solution into the physical plane to yield the temperature distribution along the impingement plate.

INTRODUCTION

A possible technique for localized cooling is to use a jet impinging against the heat-transfer surface. Liquid metals are very effective heat-transfer fluids and hence may prove useful in critical cooling applications.

For a liquid metal the molecular diffusion of heat is much larger than the molecular diffusion of momentum (low Prandtl number fluid), and hence for developing flow and heat transfer the viscous boundary layers are much thinner than the thermal boundary layers. As a result, the assumption is often made that the viscous-layer development

can be neglected in computing the heat transfer. The velocity field within the jet region can then be determined by using the techniques of inviscid free jet theory. For a two-dimensional situation in Cartesian coordinates the free streamlines can be found by conformal mapping (refs. 1 and 2). For an axisymmetric jet, numerical techniques are used (refs. 3 and 4). The present study is limited to two dimensions in Cartesian coordinates (a slot jet) so that an analytical solution can be found.

In the conformal mapping solution the two-dimensional jet flow region is mapped into a potential plane where it occupies a simple region, namely, a strip of constant height and infinite length. The convective energy equation and boundary conditions can be transformed into potential coordinates and in this coordinate system can be solved by available analytical techniques. This coordinate transformation of the energy equation has been used to determine the heat transfer for bodies in crossflow (ref. 5). The present analysis is a combination of the inviscid free jet analysis and the energy equation transformation technique. In the present problem these techniques reduce the analysis to obtaining the temperature distribution in a slab of uniform thickness moving across a plane of distributed heat sources. The solution can be found by generalizing a case treated in reference 6.

Results are obtained for the wall temperature and heat-transfer coefficient along the impingement plate for various values of the Peclet number. Simple approximate relations are obtained at the stagnation point. The stagnation results are compared with those in reference 7, which treats gases and ordinary liquids by use of a boundary-layer type of analysis.

SYMBOLS

b	half-width of undisturbed jet
C_p	specific heat of fluid
h	local heat-transfer coefficient along plate
K_n	modified Bessel function of second kind of order n
k	thermal conductivity of fluid
m	integer
Nu	Nusselt number, h2b/k
Pe	Peclet number, $\lvert v_\infty \rvert 2b/\alpha$
Pr	Prandtl number, $C_p\mu/k$

q_w heat flux specified at wall

Re jet Reynolds number, $|v_\infty| 2b\rho/\mu$

T dimensionless temperature, tk/bq_w

t temperature

U dimensionless velocity in x direction, $u/|v_\infty|$

$\vec{U}$ dimensionless fluid velocity vector, $\vec{u}/|v_\infty|$

$\vec{u}$ fluid velocity vector

u, v velocities in x and y directions

X, Y dimensionless coordinates, x/b and y/b

x, y rectangular coordinates along and normal to plate

α thermal diffusivity, $k/\rho C_p$

Γ gamma function

η dummy variable of integration

μ fluid viscosity

ν fluid kinematic viscosity, μ/ρ

ξ coordinate normal to Φ - Ψ plane

ρ fluid density

Φ dimensionless potential, $\varphi/|v_\infty|b$

φ potential function

Ψ dimensionless stream function, $\psi/|v_\infty|b$

ψ stream function

Subscripts:

w at wall

∞ undisturbed fluid condition

ANALYSIS

Geometry

The two-dimensional flow configuration is shown in figure 1. A slot jet with an undisturbed width 2b impinges normally against a flat plate at y = 0. The plate has a

uniform heat flux q_w supplied along it. After turning, the flow moves out in the positive and negative x directions in a symmetric fashion and for the inviscid-irrotational situation considered here reaches an asymptotic thickness b. From symmetry, only the first quadrant of the flow need be considered. In figure 1 some of the boundary points have been numbered 1 to 5 for convenience in identification.

Governing Equations

The fluid considered in this report is a liquid metal, and since liquid metals have very low Prandtl numbers, the viscous diffusion is small compared with the molecular diffusion of heat. Hence, in a flow where both the viscous and thermal boundary layers are developing simultaneously, there will be little diffusion of vorticity into the thermal-boundary-layer region. The viscous layer will be relatively thin, and the thermal layer will be essentially all in the inviscid region. A flow that is initially irrotational will develop little vorticity and hence can be assumed to remain irrotational. It is also assumed that the jet Reynolds number is low enough so that turbulent heat diffusion is not important in comparison with the molecular diffusion of heat, which is large for a liquid metal. These are standard assumptions for liquid-metal heat-transfer analyses in the low Reynolds number range ($RePr < 50$ in a tube or <500 for crossflow over tube bundles), as discussed in reference 8, page 300.

With these assumptions the fluid velocity can be obtained as the gradient of a potential

$$\vec{u} = \nabla \varphi \tag{1}$$

where φ is governed by Laplace's equation,

$$\nabla^2 \varphi = 0 \tag{2}$$

The Cauchy-Riemann equations apply so that the velocity components are related to the stream function by

$$u = \frac{\partial \varphi}{\partial x} = \frac{\partial \psi}{\partial y} \tag{3a}$$

$$v = \frac{\partial \varphi}{\partial y} = -\frac{\partial \psi}{\partial x} \tag{3b}$$

where the stream function also satisfies Laplace's equation,

$$\nabla^2\psi = 0 \tag{4}$$

The energy equation for the flow is given by

$$\rho C_p \vec{u} \cdot \nabla t = k\nabla^2 t \tag{5}$$

or, when equation (1) is used, by

$$\rho C_p \nabla\varphi \cdot \nabla t = k\nabla^2 t \tag{6}$$

Boundary Conditions

In connection with equations (2) and (4) governing the flow, the φ and ψ must be specified along the boundaries. Along the axis of symmetry $\widehat{34}$, the u component is zero, and along the x axis $\widehat{45}$ the v component is zero. The entire boundary $\widehat{345}$ will arbitrarily be designated as the zero streamline. These conditions give

$$\left.\begin{aligned} \frac{\partial\varphi}{\partial x} &= 0 \\ \psi &= 0 \end{aligned}\right\} \quad x = 0, \qquad y \geq 0 \tag{7a}$$

$$\left.\begin{aligned} \frac{\partial\varphi}{\partial y} &= 0 \\ \psi &= 0 \end{aligned}\right\} \quad 0 \leq x \leq \infty, \qquad y = 0 \tag{7b}$$

Along the free streamline $\widehat{12}$ the pressure is constant, since the jet is exposed to an external region at constant pressure. Consequently, the velocity magnitude along $\widehat{12}$ is equal to $|v_\infty|$. The magnitude of the stream function along $\widehat{12}$ is found by noting that the difference between this stream function and the value $\psi = 0$ on the zero streamline must equal the volume flow. Hence, along the free streamline the conditions for φ and ψ are

$$\left(\frac{\partial\varphi}{\partial x}\right)^2 + \left(\frac{\partial\varphi}{\partial y}\right)^2 = v_\infty^2 \qquad x, y \text{ on } \widehat{12} \tag{8a}$$

$$\psi = v_\infty b \qquad x, y \text{ on } \widehat{12} \tag{8b}$$

Across the width of the undisturbed incoming jet the velocity has a uniform value $-v_\infty$. Hence, from equations (3a) and (3b),

$$\left.\begin{aligned} \frac{\partial \varphi}{\partial x} &= 0 \\ \frac{\partial \psi}{\partial x} &= v_\infty \end{aligned}\right\} \quad x, y \text{ on } \widehat{23} \tag{9}$$

At large x the velocity is uniform ($u = v_\infty$, $v = 0$), so that

$$\left.\begin{aligned} \frac{\partial \psi}{\partial y} &= v_\infty \\ \frac{\partial \varphi}{\partial y} &= 0 \end{aligned}\right\} \tag{10}$$

The thermal boundary conditions are the following. There is symmetry of the temperature distribution about the axis $\widehat{34}$ so that

$$\frac{\partial t}{\partial x} = 0 \qquad x = 0, \; y \geq 0 \tag{11}$$

It is assumed that along the free streamline there is negligible heat loss so that

$$\hat{n}_s \cdot \nabla t = 0 \qquad x, y \text{ on } \widehat{12} \tag{12}$$

Along the solid boundary there is an imposed uniform heat flux q_w so that

$$\frac{\partial t}{\partial y} = -\frac{q_w}{k} \qquad 0 \leq x \leq \infty, \; y = 0 \tag{13}$$

Along the cross section of the incoming undisturbed jet the fluid is at uniform temperature t_∞:

$$t = t_\infty \qquad x, y \text{ on } \widehat{23} \tag{14}$$

Equations and Boundary Conditions in Dimensionless Form

The preceding equations and boundary conditions can be placed in dimensionless form by defining the following variables:

$$\left.\begin{aligned} X &= \frac{x}{b} & \tilde{\nabla} &= b\nabla \\ Y &= \frac{y}{b} & \Phi &= \frac{\varphi}{|v_\infty| b} \\ \vec{U} &= \frac{\vec{u}}{|v_\infty|} & \Psi &= \frac{\psi}{|v_\infty| b} \\ T &= \frac{tk}{bq_w} & Pe &= \frac{|v_\infty| 2b}{\alpha} \end{aligned}\right\} \tag{15}$$

The flow and energy equations (1), (2), and (6) become

$$\vec{U} = \tilde{\nabla}\Phi \tag{16}$$

$$\tilde{\nabla}^2\Phi = 0 \tag{17}$$

$$\frac{Pe}{2}\,\tilde{\nabla}\Phi \cdot \tilde{\nabla}T = \tilde{\nabla}^2 T \tag{18}$$

The boundary conditions are

$$\left.\begin{aligned} &\frac{\partial\Phi}{\partial X} = 0 \\ &\Psi = 0 \\ &\frac{\partial T}{\partial X} = 0 \end{aligned}\right\} \quad x = 0,\ y \geq 0 \qquad (x, y \text{ on } \widehat{34}) \tag{19}$$

$$\left.\begin{aligned} \frac{\partial \Phi}{\partial Y} &= 0 \\ \Psi &= 0 \\ \frac{\partial T}{\partial Y} &= -1 \end{aligned}\right\} \quad 0 \leq x \leq \infty, \; y = 0 \qquad (x, y \text{ on } \widehat{45}) \tag{20}$$

$$\left.\begin{aligned} \left(\frac{\partial \Phi}{\partial X}\right)^2 + \left(\frac{\partial \Phi}{\partial Y}\right)^2 &= 1 \\ \Psi &= 1 \\ \hat{n}_s \cdot \tilde{\nabla} T &= 0 \end{aligned}\right\} \quad x, y \text{ on } \widehat{12} \tag{21}$$

$$\left.\begin{aligned} \frac{\partial \Phi}{\partial X} &= 0 \\ \frac{\partial \Psi}{\partial X} &= 1 \\ T &= T_\infty \end{aligned}\right\} \quad x, y \text{ on } \widehat{23} \tag{22}$$

$$\left.\begin{aligned} \frac{\partial \Psi}{\partial Y} &= 1 \\ \frac{\partial \Phi}{\partial Y} &= 0 \end{aligned}\right\} \quad x, y \text{ on } \widehat{15} \tag{23}$$

Solution of Flow Problem

The solution for an inviscid two-dimensional jet slot jet striking a plane is available in many textbooks as an example of conformal mapping applied to free jet theory. In the course of the solution the jet is transformed into a potential plane as shown in figure 2. In this plane the flow has a uniform velocity and is from left to right in a two-dimensional channel of unit height. The mapping functions relating the potential and physical planes can be obtained as a special case of the results in reference 9.

The heated plate $\widehat{45}$ in figure 1 is along the positive Φ axis ($\Psi = 0$) in figure 2. The locations along the positive Φ axis are of interest here, as it is the heat-transfer behavior along the plate that is desired. From the results in reference 9 the correspondence between Φ and X is given by

$$\left.\begin{aligned} \Phi\big|_{\Psi=0} &= \frac{2}{\pi} \ln \frac{1+U^2}{1-U^2} \\ X\big|_{\Psi=0} &= \frac{2}{\pi}\left(2 \tan^{-1} U + \ln \frac{1+U}{1-U}\right) \end{aligned}\right\} \quad 0 \le U \le 1 \tag{24}$$

where U is the dimensionless velocity in the physical plane along the plate in the x direction. The results in equation (24) are all that will be needed from the flow portion of the problem.

Formulation for Solution of Energy Equation by Use of Potential Plane

The strip region in figure 2 is a simple geometry, and hence it provides a convenient region in which to solve the energy equation. The solution can be evaluated along the boundary $\widehat{45}$ in figure 2, where the quantities of interest are functions of Φ. Equation (24) can then be used to find the corresponding X values so that the heat-transfer behavior is obtained along the plate in the physical plane.

The energy equation, equation (18), has the same form as that of equation (16) of reference 10, and this reference gives the details of the transformation from X, Y to Φ, Ψ coordinates. Using equation (26) of reference 10 yields the energy equation

$$\frac{\partial^2 T}{\partial \Phi^2} + \frac{\partial^2 T}{\partial \Psi^2} - \frac{Pe}{2} \frac{\partial T}{\partial \Phi} = 0 \tag{25}$$

This is the same energy equation as for convection to a flow with uniform velocity in a parallel-plate channel. The flow would be in the Φ direction with the channel width extending across the Ψ direction.

The temperature boundary conditions in equations (19) to (22) must also be expressed in terms of Φ and Ψ. Equation (19) expresses symmetry about the jet axis. This symmetry is preserved in the transformed plane so that the condition becomes

$$\frac{\partial T}{\partial \Psi} = 0 \qquad \Phi, \Psi \quad \text{on } \widehat{34} \tag{26}$$

To transform equation (20) use the relation that at a fixed X

$$\frac{\partial T}{\partial Y} = \frac{\partial T}{\partial \Psi}\frac{\partial \Psi}{\partial Y} + \frac{\partial T}{\partial \Phi}\frac{\partial \Phi}{\partial Y}$$

Applying the conditions from equation (20) along $\Psi = 0$ gives

$$-1 = \left.\frac{\partial T}{\partial \Psi}\right|_{\Psi=0} \left.\frac{\partial \Psi}{\partial Y}\right|_{\Psi=0}$$

From equation (3a)

$$U = \frac{\partial \Psi}{\partial Y}$$

Hence, the boundary condition becomes

$$\frac{\partial T}{\partial \Psi} = -\frac{1}{U(\Phi)} \qquad \Phi, \Psi \quad \text{on } \widehat{45} \tag{27}$$

where from equation (24)

$$U(\Phi) = \left(\frac{e^{\pi\Phi/2} - 1}{e^{\pi\Phi/2} + 1}\right)^{1/2} = \left(\tanh \frac{\pi\Phi}{4}\right)^{1/2}$$

Since the free streamline $\widehat{12}$ is a line of constant Ψ, the condition equation (21) becomes

$$\frac{\partial T}{\partial \Psi} = 0 \qquad \Phi, \Psi \quad \text{on } \widehat{12} \tag{28}$$

From equation (22)

$$T = T_\infty \qquad \Phi, \Psi \quad \text{on } \widehat{23} \tag{29}$$

These boundary conditions are summarized in figure 2.

In the potential plane (fig. 2) the situation is a channel flow with uniform velocity (i.e., a moving slab) and a uniform entering fluid temperature T_∞. Equation (25) is the convection equation with the axial conduction term $\partial^2 T/\partial \Phi^2$ included. The channel boundary conditions correspond to insulated walls except for a nonuniform heat addition along the positive Φ axis. The solution can be obtained by utilizing some results from reference 6. The desired result is the temperature distribution along the plate that the jet is impinging against. This can also be expressed in terms of a local Nusselt number along the plate. The local heat-transfer coefficient is $h = q_w/(t_w - t_\infty)$. Then the local Nusselt number based on the jet width 2b is

$$\mathrm{Nu}(X) = \frac{h2b}{k} = \frac{q_w 2b}{(t_w - t_\infty)k} = \frac{2}{T_w(X) - T_\infty} \tag{30}$$

Solution of Energy Equation

Equation (8) on page 268 of reference 6 gives the temperature on the surface of a slab that is moving past a line source of heat. If superposition is used to obtain the effect of a distribution of line sources, the solution can be found for the present problem. A difficulty is that the result given in reference 6 is valid only for positive distances along the surface away from the line source. A relation valid for both positive and negative distances is needed to superpose the line sources and obtain a continuous source distribution as given by $-1/U(\Phi)$ in figure 2. The details of the solution are given in appendix A, and the final result for the wall temperature along the positive Φ axis (segment $\widehat{45}$) is given by

$$T_w(\Phi) - T_\infty = \frac{2}{Pe}\left[\int_{\eta=0}^{\Phi} \frac{d\eta}{\left(\tanh\frac{\pi\eta}{4}\right)^{1/2}} + \int_{\eta=\Phi}^{\infty} \frac{e^{-(Pe/2)(\eta-\Phi)}}{\left(\tanh\frac{\pi\eta}{4}\right)^{1/2}}\, d\eta \right.$$

$$+ \sum_{m=1}^{\infty} \frac{2}{\left[1+\left(\frac{4m\pi}{Pe}\right)^2\right]^{1/2}} \left(\int_{\eta=0}^{\Phi} \frac{e^{(Pe/4)(\Phi-\eta)\left\{1-\left[1+(4m\pi/Pe)^2\right]^{1/2}\right\}}}{\left(\tanh\frac{\pi\eta}{4}\right)^{1/2}}\, d\eta \right.$$

$$\left. \left. + \int_{\eta=\Phi}^{\infty} \frac{e^{-(Pe/4)(\eta-\Phi)\left\{1+\left[1+(4m\pi/Pe)^2\right]^{1/2}\right\}}}{\left(\tanh\frac{\pi\eta}{4}\right)^{1/2}}\, d\eta \right) \right] \tag{31}$$

Equation (24) is then used to transform from Φ to X, and $T_w(X) - T_\infty$ can then be plotted along the impingement plate. The expression has been evaluated by numerical integration, and results are given in figure 3(a) for Pe = 5, 10, 20, and 50. The local Nusselt number is obtained from equation (30) and is plotted in figure 4(a).

Simplified Solution Neglecting Axial Conduction

In channel-flow heat-transfer analyses (ref. 11), the neglect of axial conduction produces only a small error for Pe between 10 and 100, and for Pe > 100 the error is negligible. Hence, it is worthwhile to examine here an approximate solution for which the axial conduction (conduction along the streamlines when transformed back into the jet geometry) is neglected. Compared with equation (31), this provides a much more simple solution that is convenient to evaluate and is accurate when Pe is sufficiently large. With this assumption the energy equation (25) simplifies to

$$\frac{\partial^2 T}{\partial \Psi^2} - \frac{Pe}{2}\frac{\partial T}{\partial \Phi} = 0 \tag{32}$$

which is of the same form as the transient-heat-conduction equation. The boundary condition (29) now applies along the axis $\Phi = 0$. The problem is the same as that for a plate of unit thickness that is initially at uniform temperature and that has one boundary kept insulated and one boundary with a heat input that varies with time. The solution can be obtained by using a superposition in time of the uniform-heat-flux solution in equation (4) on page 112 of reference 6. The derivation is given in appendix B with the result that the wall temperature is given by

$$T_w(\Phi) - T_\infty = \left(\frac{2}{\pi Pe}\right)^{1/2} \int_0^{\Phi} \frac{1}{\left[\eta \tanh \frac{\pi(\Phi - \eta)}{4}\right]^{1/2}} \sum_{m=0}^{\infty} \left[e^{-(Pe/2\eta)m^2} + e^{-(Pe/2\eta)(m+1)^2}\right] d\eta \tag{33}$$

Equation (24) is used to obtain Φ values corresponding to the desired X values, and the $T_w(X)$ are then evaluated by numerically integrating equation (33) for these Φ. The wall temperature distribution and corresponding Nusselt number distribution are plotted in figures 3(a) and 4(a) for various Pe.

Simplified Solution Neglecting Axial Conduction and Upper Boundary

The heat transfer in the vicinity of the stagnation region is sufficiently distant from the jet free streamlines that it is worth considering the solution of the energy equation where the effect of the upper boundary in figure 2 is neglected. As explained in the previous section, the solution with axial conduction neglected is then the same as the solution for the transient-heat-conduction equation - in this instance for a semi-infinite region. From reference 6 (p. 76, eq. (9)) the solution for T_w can be written as

$$T_w(\Phi) - T_\infty = \left(\frac{2}{\pi Pe}\right)^{1/2} \int_0^{\Phi} \frac{i}{U(\Phi - \eta)} \frac{d\eta}{\eta^{1/2}}$$

Inserting the $U(\Phi)$ for the jet configuration as given by equation (27) gives

$$T_w(\Phi) - T_\infty = \left(\frac{2}{\pi Pe}\right)^{1/2} \int_0^\Phi \frac{1}{\left[\eta \tanh \frac{\pi(\Phi - \eta)}{4}\right]^{1/2}} d\eta \tag{34}$$

The solution is thus a simplified form of equation (33) in which the infinite series accounted for the effect of the opposite wall.

It is useful to evaluate equation (34) at the stagnation point as this is the region of highest heat transfer. As $\Phi \to 0$ in this equation, the η and $\Phi - \eta$ will always be very small. For a small argument the hyperbolic tangent equals the argument, so equation (34) becomes for small Φ

$$T_w(\Phi \to 0) - T_\infty = \left(\frac{2}{\pi Pe}\right)^{1/2} \int_0^\Phi \frac{d\eta}{\left[\eta \frac{\pi(\Phi - \eta)}{4}\right]^{1/2}} = \frac{2}{\pi} \sqrt{\frac{2}{Pe}} \int_0^\Phi \frac{d\eta}{\left[\eta(\Phi - \eta)\right]^{1/2}}$$

Let $\overline{\eta} = \eta/\Phi$ to obtain

$$T_w(\Phi \to 0) - T_\infty = \frac{2}{\pi} \sqrt{\frac{2}{Pe}} \int_0^1 \frac{d\overline{\eta}}{\left[\overline{\eta}(1 - \overline{\eta})\right]^{1/2}}$$

and then let $\beta = \overline{\eta}^{1/2}$ to yield

$$T_w(\Phi \to 0) - T_\infty = \frac{2}{\pi} \sqrt{\frac{2}{Pe}} \int_0^1 \frac{2d\beta}{\sqrt{1 - \beta^2}} = \frac{4}{\pi} \sqrt{\frac{2}{Pe}} \sin^{-1}\beta \Big|_0^1 = \frac{4}{\pi} \sqrt{\frac{2}{Pe}} \frac{\pi}{2} = 2 \sqrt{\frac{2}{Pe}} \tag{35}$$

From equation (30)

$$\mathrm{Nu}(\Phi \to 0) = \frac{2}{2\sqrt{\frac{2}{\mathrm{Pe}}}} = \sqrt{\frac{\mathrm{Pe}}{2}} \tag{36}$$

Limiting Values for Large Values of Dimensionless Coordinate X

For large X it is possible to obtain a simple limiting solution. From figure 1 it is evident that for large X the situation is a channel flow, and with viscous effects neglected, the velocity is uniform. The channel is bounded at the top by the free streamline, which is assumed insulated, and at the bottom by the plate, which has a uniform heat addition. This region is treated as a channel flow in appendix C, and the result for the wall temperature at large X is

$$T_w(X) - T_\infty = \frac{2}{\mathrm{Pe}} X + \frac{1}{3} \tag{37}$$

This is compared with the solutions with and without axial conduction in figures 3(a) and 4(a).

DISCUSSION

The condition considered here is for the impingement plate being heated uniformly, and the analysis yields the temperature distribution along the plate. The results are shown in figure 3; part (a) gives the temperature distribution along the plate, and part (b) gives the value at the stagnation point. The solid curves are the exact solution as given by equation (31), and as is typical of liquid metals, the results depend only on the single parameter Pe which does not involve viscosity. Numerical values are given in table I. As expected for a stagnation type flow, the highest heat transfer is at the stagnation point, and this is shown by the wall temperature being lowest at X = 0. The convective heat transfer should increase with the value of Pe, and the manner of this increase is revealed in figure 3. The heat-transfer characteristics can also be expressed in the form of a local Nusselt number which is a reciprocal relation to the wall temperature, as shown by equation (30). The Nusselt number distribution along the plate and the stagnation Nusselt number are shown in figures 4(a) and (b).

An increase in convection, which corresponds to an increase in Peclet number, should diminish the effect of conduction along the streamlines, and the solution in equation (33) should then apply. This relation is plotted as the long-dash curves in figures 3(a) and 4(a). It is evident that the conduction term can be neglected, and the error will be within a few percent for Pe greater than about 10. Hence, unless Pe is somewhat lower than 10, it is unnecessary to evaluate the exact solution as the simpler equation (33) will suffice.

At stagnation the neglect of the upper boundary and conduction along the streamlines leads to the following simple relations from equations (35) and (36):

$$T_w(X=0) - T_\infty = 2\sqrt{\frac{2}{Pe}} \tag{38a}$$

$$Nu(X=0) = \sqrt{\frac{Pe}{2}} \tag{38b}$$

As shown by the curves in figures 3(b) and 4(b), these relations are very good approximations for $Pe > 10$. For low Pe the conduction along the streamlines at stagnation decreases the heat transfer somewhat, as evidenced by the exact solution in figure 4(b) being below the solution neglecting heat conduction. Heat is conducted upstream into the flow as it approaches the plate, and this tends to thicken the thermal boundary layer near stagnation and decrease the heat transfer. Figure 3 shows that the wall temperature is fairly uniform in the vicinity of stagnation. Hence, the stagnation results in equations (38) should also apply for the boundary condition of uniform wall temperature.

Equation (37) provides a simple asymptotic result for large X. The results show that this is a good approximation for X larger than about 6 with Pe greater than about 10. At smaller X the asymptotic solution begins to deviate gradually from the exact results, and the approximation is not very good for X less than about 4 for the Pe values considered in this report.

The analysis in reference 7 is concerned with gases and liquids, $0.7 \leq Pr \leq 10$, rather than the low Prandtl number range typical of liquid metals in the present report. The boundary condition at the impingement plate in reference 7 is a specified uniform wall temperature rather than a uniform heat flux like that treated in this report. For $0 \leq Pr \leq 10$ the viscous boundary layer is almost as thick or is thicker than the thermal layer, so that a boundary-layer analysis for the flow is required. The solution is obtained numerically with the jet potential flow solution used for the external flow. The analysis also includes the jet nozzle being at various distances from the plate. For large nozzle distances from the plate, as in the present report, the variations of Nusselt number along the plate have the same general trends as those obtained in this report.

At the stagnation point the correlation obtained in reference 7 is $Nu = 0.51\ Re^{1/2}Pr^{0.373}$ as compared with $Nu = 0.707\ Pe^{1/2} = 0.707(RePr)^{1/2}$ for the present report. The correlation in reference 7 can be rearranged into $Nu = 0.51(RePr)^{1/2}/Pr^{0.127} = 0.51\ Pe^{1/2}/Pr^{0.127}$. Viscosity appears only in the Prandtl number, and since the Prandtl number is to a small power, the heat-transfer behavior at the stagnation point is not very viscosity dependent.

CONCLUSIONS

An analysis has been performed combining free jet theory and a transformation of the energy equation into the potential plane to obtain the heat-transfer behavior of an impinging liquid-metal jet. The jet is two-dimensional in Cartesian coordinates and strikes a plate that is uniformly heated. The temperature distribution and heat-transfer coefficient are evaluated along the plate as a function of the Peclet number Pe. As would be expected, the maximum heat-transfer coefficient is at the stagnation point. At a distance larger than about 6 jet half-widths from stagnation and for $Pe > 10$, the results can be approximated quite well by an asymptotic relation that considers the jet region to act like a channel flow. Heat conduction along the streamlines is not very significant when Pe is greater than 10. For this Pe range, the Nusselt number Nu at stagnation can be approximated quite well by $Nu = \sqrt{Pe/2}$. This result should also apply for the boundary condition of uniform wall temperature because the present solution yielded almost uniform wall temperatures in the vicinity of stagnation.

Lewis Research Center,
National Aeronautics and Space Administration,
Cleveland, Ohio, February 7, 1973,
501-24.

APPENDIX A

SOLUTION OF ENERGY EQUATION

The solution can be obtained by starting with the equation for a stationary point source of heat on one side of a moving slab with the other side of the slab insulated. By superposition the point source is used to obtain the solution for a line source. Then a superposition of line sources can be used to build up the heat source distribution specified by the boundary condition equation (27) along the positive axis.

For a slab of unit thickness, $0 < \Psi < 1$, moving with a unit velocity (fig. 2) the temperature distribution produced by a unit point heat source fixed at the origin, $\Phi = \Psi = \xi = 0$ (the ξ is a coordinate axis perpendicular to Φ and Ψ), is obtained from reference 6, page 268, equation (7), as

$$T(\Phi, \Psi) - T_\infty = \frac{1}{2\pi}\left(K_0\left(\frac{Pe}{4}\sqrt{\Phi^2 + \xi^2}\right) + 2\sum_{m=1}^{\infty} K_0\left\{\left(\frac{Pe}{4}\sqrt{\Phi^2 + \xi^2}\right)\left[1 + \left(\frac{4}{Pe}\right)^2 m^2\pi^2\right]^{1/2}\right\}\cos(m\pi\Psi)\right) e^{\Phi Pe/4} \tag{A1}$$

Integrating over ξ yields the temperature distribution for a line source along the ξ axis

$$T(\Phi, \Psi) - T_\infty = \frac{1}{2\pi}\int_{\xi=-\infty}^{\xi=+\infty}\left(K_0\left(\frac{Pe}{4}\sqrt{\Phi^2 + \xi^2}\right) + 2\sum_{m=1}^{\infty} K_0\left\{\left(\frac{Pe}{4}\sqrt{\Phi^2 + \xi^2}\right)\left[1 + \left(\frac{4}{Pe}\right)^2 m^2\pi^2\right]^{1/2}\right\}\cos(m\pi\Psi)\right) e^{\Phi Pe/4}\, d\xi \tag{A2}$$

To carry out this integration the result from reference 12, page 417, is used that

$$\int_0^\infty \frac{K_\nu\left(a\sqrt{t^2+\zeta^2}\right)}{\left(t^2+\zeta^2\right)^{(1/2)\nu}} t^{2\mu+1}\,dt = \frac{2^\mu \Gamma(\mu+1)}{a^{\mu+1}\zeta^{\nu-\mu-1}} K_{\nu-\mu-1}(a\zeta) \qquad a > 0 \tag{A3}$$

Since the integrand in equation (A3) contains only ζ^2, the result should be the same for negative ζ as for positive ζ. Hence, to allow for negative ζ the result in equation (A3) should more properly be written as

$$\int_0^\infty \frac{K_\nu\left(a\sqrt{t^2+\zeta^2}\right)}{\left(t^2+\zeta^2\right)^{(1/2)\nu}} t^{2\mu+1}\,dt = \frac{2^\mu \Gamma(\mu+1)}{a^{\mu+1}|\zeta|^{\nu-\mu-1}} K_{\nu-\mu-1}(a|\zeta|) \tag{A4}$$

A specific case for $\nu = 0$ and $\mu = -1/2$ is

$$\int_0^\infty K_0\left(a\sqrt{t^2+\zeta^2}\right)dt = \frac{1}{\sqrt{2}} \frac{\Gamma\left(\frac{1}{2}\right)|\zeta|^{1/2}}{a^{1/2}} K_{-1/2}(a|\zeta|)$$

Using the relations $K_{-1/2} = K_{1/2}$, $\Gamma(1/2) = \sqrt{\pi}$, and $\sqrt{(\pi/2\zeta)}\,K_{1/2}(\zeta) = (\pi/2\zeta)\,e^{-\zeta}$ (see ref. 13, p. 444) yields the simplified form

$$\int_0^\infty K_0\left(a\sqrt{t^2+\zeta^2}\right)dt = \frac{\pi}{2a} e^{-a|\zeta|} \tag{A5}$$

From symmetry equation (A2) can be written with integration limits $0 \to \infty$ as

$$T_w - T_\infty = \frac{1}{\pi}\int_0^\infty \left(K_0\left(\frac{Pe}{4}\sqrt{\Phi^2+\xi^2}\right) + 2\sum_{m=1}^{\infty} K_0\left\{\left(\frac{Pe}{4}\sqrt{\Phi^2+\xi^2}\right)\left[1+\left(\frac{4}{Pe}\right)^2 m^2\pi^2\right]^{1/2}\right\}\cos(m\pi\Psi)\right) e^{\Phi Pe/4}\,d\xi \tag{A6}$$

Equation (A6) is integrated by use of equation (A5) to yield

$$T(\Phi, \Psi) - T_\infty = \frac{1}{\pi}\left\{\frac{\pi}{2}\frac{4}{Pe}e^{-(Pe/4)|\Phi|} + 2\sum_{m=1}^{\infty}\frac{\frac{\pi}{2}\,e^{-(Pe/4)\left[1+(4m\pi/Pe)^2\right]^{1/2}|\Phi|}}{\frac{Pe}{4}\left[1+\left(\frac{4}{Pe}\right)^2 m^2\pi^2\right]^{1/2}}\cos(m\pi\Psi)\right\}e^{\Phi Pe/4}$$

Simplifying and evaluating at the wall $\Psi = 0$ give

$$T_w(\Phi) - T_\infty = \frac{2}{Pe}\left(e^{(Pe/4)(\Phi-|\Phi|)} + \sum_{m=1}^{\infty}\frac{2}{\left[1+\left(\frac{4m\pi}{Pe}\right)^2\right]^{1/2}}e^{(Pe/4)\left\{\Phi-|\Phi|\left[1+(4m\pi/Pe)^2\right]^{1/2}\right\}}\right) \tag{A7}$$

Equation (A7) gives the wall-temperature distribution produced by a line source of unit strength per unit length along the ξ axis in figure 2. Superposition can now be

applied along the positive Φ axis to obtain the effect of the source distribution $1/U(\Phi)$ which resulted from the imposed uniform heat flux in the physical plane being transformed into the potential plane. If $H(\Phi)$ is the response to a unit line source, and $F(\Phi)$ is the distribution of sources, the wall-temperature distribution can be obtained by superposition as

$$T_w(\Phi) - T_\infty = \int_{\eta=0}^{\infty} F(\eta)H(\Phi - \eta)\, d\eta \tag{A8}$$

Using equation (A7) for $H(\Phi)$ gives

$$T_w(\Phi) - T_\infty = \frac{2}{Pe} \int_{\eta=0}^{\infty} \frac{1}{U(\eta)} \left(e^{(Pe/4)(\Phi-\eta-|\Phi-\eta|)} + \sum_{m=1}^{\infty} \frac{2}{\left[1 + \left(\frac{4m\pi}{Pe}\right)^2\right]^{1/2}} e^{(Pe/4)\left\{(\Phi-\eta)-|\Phi-\eta|\left[1+(4m\pi/Pe)^2\right]^{1/2}\right\}} \right) d\eta \tag{A9}$$

The $U(\eta)$ is inserted from equation (27) and the integral is divided into two regions depending on whether $\eta < \Phi$ or $\eta > \Phi$ to obtain the final form

$$T_w(\Phi) - T_\infty = \frac{2}{Pe}\left[\int_{\eta=0}^{\Phi} \frac{d\eta}{\left(\tanh\frac{\pi\eta}{4}\right)^{1/2}} + \int_{\eta=\Phi}^{\infty} \frac{e^{-(Pe/2)(\eta-\Phi)}}{\left(\tanh\frac{\pi\eta}{4}\right)^{1/2}}\, d\eta\right.$$

$$+ \sum_{m=1}^{\infty} \frac{2}{\left[1+\left(\frac{4m\pi}{Pe}\right)^2\right]^{1/2}}\left(\int_{\eta=0}^{\Phi} \frac{e^{(Pe/4)(\Phi-\eta)\left\{1-\left[1+(4m\pi/Pe)^2\right]^{1/2}\right\}}}{\left(\tanh\frac{\pi\eta}{4}\right)^{1/2}}\, d\eta\right.$$

$$\left.\left. + \int_{\eta=\Phi}^{\infty} \frac{e^{-(Pe/4)(\eta-\Phi)\left\{1+\left[1+(4m\pi/Pe)^2\right]^{1/2}\right\}}}{\left(\tanh\frac{\pi\eta}{4}\right)^{1/2}}\, d\eta\right)\right] \qquad \text{(A10)}$$

APPENDIX B

SOLUTION NEGLECTING AXIAL CONDUCTION

In reference 6, page 112, the transient temperature solution is given for a heat flux suddenly imposed at one surface of a slab with the other surface of the slab insulated. Since equation (32) has the same form as the transient heat conduction equation, this solution can be applied after changing the nomenclature. The Φ is analogous to time in the transient problem, and since the heat flux varies with Φ in the present case, the solution is the same as a transient solution in which the imposed heat flux varies with time. The superposition theorem for the variable-heat-flux solution is

$$T_w(\Phi) - T_\infty = \int_0^\Phi \frac{1}{U(\Phi - \eta)} \frac{dF}{d\eta} \, d\eta \tag{B1}$$

where $1/U(\Phi)$ is given by equation (27), and F is the response to a suddenly imposed heat flux of unit magnitude.

From the solution in reference 6 the F is given by

$$F(\Phi) = 2\left(\frac{2\Phi}{Pe}\right)^{1/2} \sum_{m=0}^{\infty} \left\{ \text{ierfc}\left[\frac{m}{\left(\frac{2}{Pe}\Phi\right)^{1/2}}\right] + \text{ierfc}\left[\frac{m+1}{\left(\frac{2}{Pe}\Phi\right)^{1/2}}\right] \right\}$$

where

$$\text{ierfc}\,\xi = \frac{1}{\sqrt{\pi}} e^{-\xi^2} - \xi \,\text{erfc}\,\xi$$

The derivative of this function is given by

$$\frac{d}{d\Phi} \text{ierfc}\,\xi = \frac{d(\text{ierfc}\,\xi)}{d\xi} \frac{d\xi}{d\Phi} = (-\text{erfc}\,\xi) \frac{d\xi}{d\Phi}$$

Using this relation gives

$$\frac{dF}{d\Phi} = \left(\frac{2}{\Phi Pe}\right)^{1/2} \sum_{m=0}^{\infty} \left\{ \text{ierfc}\left[\frac{m}{\left(\frac{2}{Pe}\Phi\right)^{1/2}}\right] + \text{ierfc}\left[\frac{m+1}{\left(\frac{2}{Pe}\Phi\right)^{1/2}}\right] \right\} + \left(\frac{2\Phi}{Pe}\right)^{1/2} \sum_{m=0}^{\infty} \left\{ \frac{m}{\Phi\left(\frac{2}{Pe}\Phi\right)^{1/2}} \text{erfc}\left[\frac{m}{\left(\frac{2}{Pe}\Phi\right)^{1/2}}\right] + \frac{m+1}{\Phi\left(\frac{2}{Pe}\Phi\right)^{1/2}} \text{erfc}\left[\frac{m+1}{\left(\frac{2}{Pe}\Phi\right)^{1/2}}\right] \right\} \tag{B2}$$

When the definitions of ierfc ξ and erfc ξ are used, equation (B2) reduces to

$$\frac{dF}{d\Phi} = \left(\frac{2}{\Phi Pe}\right)^{1/2} \frac{1}{\sqrt{\pi}} \sum_{m=0}^{\infty} \left[e^{-m^2/(2/Pe)\Phi} + e^{-(m+1)^2/(2/Pe)\Phi} \right] \tag{B3}$$

Substitute equation (B3) into equation (B1) and use equation (27) for U to obtain the desired final result for the wall-temperature distribution

$$T_w(\Phi) - T_\infty = \left(\frac{2}{\pi Pe}\right)^{1/2} \int_0^{\Phi} \frac{1}{\left[\eta \tanh \frac{\pi(\Phi - \eta)}{4}\right]^{1/2}} \sum_{m=0}^{\infty} \left[e^{-m^2 Pe/2\eta} + e^{-(m+1)^2 Pe/2\eta} \right] d\eta \tag{B4}$$

APPENDIX C

LIMITING HEAT TRANSFER AT LARGE VALUES OF DIMENSIONLESS COORDINATE X

For large x the flow as shown in figure 5 is a flow with uniform velocity in a channel with one wall heated and one wall insulated. An overall heat balance is now taken on the flow region from the fluid entrance at large y to the region at large x, where the velocity is uniform and equal to v_∞. This yields for large x

$$q_w x = b v_\infty \rho C_p \left[\bar{t}(x) - t_\infty\right] \tag{C1}$$

where $\bar{t}(x)$ is the mean temperature for uniform velocity (see eq. (C7)) obtained as $\bar{t}(x) = \frac{1}{b}\int_0^b t(x, y)\, dy$. Equation (C1) determines the $\bar{t}(x)$ since q_w is a specified quantity.

A heat balance on a differential element in the fluid gives

$$k\left(\frac{\partial^2 t}{\partial x^2} + \frac{\partial^2 t}{\partial y^2}\right) = v_\infty \rho C_p \frac{\partial t}{\partial x} \tag{C2}$$

For fully developed heat transfer with uniform heat addition the temperature distribution rises linearly with x and hence has the form

$$t(x, y) = C_1 x + f(y) \tag{C3}$$

The axial conduction term $k(\partial^2 t/\partial x^2)$ is thus zero, and substitution of equation (C3) into (C2) yields

$$k \frac{d^2 f}{dy^2} = v_\infty \rho C_p C_1 \tag{C4}$$

Since in the fully developed region the shape of the temperature distribution is not changing, equation (C1) yields

$$\frac{\partial t}{\partial x} = \frac{\partial \bar{t}}{\partial x} = \frac{q_w}{b v_\infty \rho C_p} = C_1 \tag{C5}$$

Then combining equations (C5) and (C4) gives

$$\frac{d^2f}{dy^2} = \frac{q_w}{kb}$$

Integrate once and apply the boundary condition that $\partial t/\partial y = \partial f/\partial y = 0$ at $y = b$ to obtain

$$\frac{df}{dy} = \frac{q_w}{kb}(y - b)$$

A second integration results in

$$f = \frac{q_w}{kb}\left(\frac{y^2}{2} - by\right) + C_2 \tag{C6}$$

The integrated average temperature is

$$\bar{t}(x) = \frac{\int_0^b ut\,dy}{\int_0^b u\,dy} = \frac{v_\infty \int_0^b t\,dy}{v_\infty \int_0^b dy} = \frac{1}{b}\int_0^b t\,dy \tag{C7}$$

Substituting for t by use of equations (C3), (C5), and (C6) gives

$$\bar{t}(x) = \frac{1}{b}\int_0^b \left[\frac{q_w x}{bv_\infty \rho C_p} + \frac{q_w}{kb}\left(\frac{y^2}{2} - by\right) + C_2\right] dy$$

$$\bar{t}(x) = \frac{1}{b}\left(\frac{q_w x}{v_\infty \rho C_p} - \frac{q_w}{kb}\frac{b^3}{3} + C_2 b\right)$$

Using $\bar{t}(x)$ from equation (C1) gives

$$\frac{q_w x}{bv_\infty \rho C_p} + t_\infty = \frac{q_w x}{bv_\infty \rho C_p} - \frac{q_w b}{3k} + C_2$$

so that

$$C_2 = t_\infty + \frac{q_w b}{3k} \tag{C8}$$

Combining equations (C3), (C5), (C6), and (C8) gives the temperature distribution

$$t = \frac{q_w x}{b v_\infty \rho C_p} + \frac{q_w}{kb}\left(\frac{y^2}{2} - by\right) + t_\infty + \frac{q_w b}{3k}$$

Evaluating at $y = 0$ to obtain the wall temperature yields

$$t_w(x) - t_\infty = \frac{q_w x}{b v_\infty \rho C_p} + \frac{q_w b}{3k}$$

In dimensionless form the final result is

$$T_w(X) - T_\infty = \frac{2}{Pe} X + \frac{1}{3} \tag{C9}$$

REFERENCES

1. Birkhoff, Garrett; and Zarantonello, E. H.: Jets, Wakes, and Cavities. Academic Press, Inc., 1957.

2. Milne-Thomson, L. M.: Theoretical Hydrodynamics. Second ed., The Macmillan Co., 1950.

3. Schach, W.: Umlenkung eines kreisförmigen Flüssigkeitsstrahles an einer ebenen Platte senkrecht zur Strömungsrichtung. Ing.-Arch., vol. 6, no. 1, 1935, pp. 51-59.

4. Saad, Michel A.; and Antonides, Gene J.: Flow Pattern of Two Impinging Circular Jets. AIAA J., vol. 10, no. 7, July 1972, pp. 929-931.

5. Grosh, R. J.; and Cess, R. D.: Heat Transfer to Fluids with Low Prandtl Numbers for Flow Across Plates and Cylinders of Various Cross Section. ASME Trans., vol. 80, no. 3, Apr. 1958, pp. 667-676.

6. Carslaw, Horatio S.; and Jaeger, J. C.: Conduction of Heat in Solids. Second ed., Oxford Univ. Press, 1959.

7. Miyazaki, H.; and Silberman, E.: Flow and Heat Transfer on a Flat Plate Normal to a Two-Dimensional Laminar Jet Issuing from a Nozzle of Finite Height. Int. J. Heat Mass Transfer, vol. 15, Nov. 1972, pp. 2097-2107.

8. Eckert, E. R. G.; and Drake, Robert M., Jr.: Heat and Mass Transfer. Second ed., McGraw-Hill Book Co., Inc., 1959.

9. Gedney, Richard T.; and Siegel, Robert: Inviscid Flow Analysis of Two Parallel Slot Jets Impinging Normally on a Surface. NASA TN D-4957, 1968.

10. Siegel, Robert; and Goldstein, Marvin E.: Analytical Method for Steady State Heat Transfer in Two-Dimensional Porous Media. NASA TN D-5878, 1970.

11. Schneider, P. J.: Effect of Axial Fluid Conduction on Heat Transfer in the Entrance Regions of Parallel Plates and Tubes. ASME Trans., vol. 79, no. 4, May 1957, pp. 765-773.

12. Watson, George N.: A Treatise on the Theory of Bessel Functions. Second ed., Cambridge Univ. Press, 1966.

13. Abramowitz, M.; and Stegun, I. A., eds.: Handbook of Mathematical Functions with Formulas, Graphs, and Mathematical Tables. Appl. Math. Ser. 55, National Bureau of Standards, June 1964 (6th Printing, 1967).

TABLE I. - WALL TEMPERATURES ALONG IMPINGEMENT PLATE

[From (eq. (31).]

Dimensionless coordinate, X	Dimensionless potential, Φ	Peclet number, Pe			
		5	10	20	50
		Wall temperature, $T_w(X) - T_\infty$			
0	0	1.324	0.893	0.630	0.397
1	.1960	1.366	.902	.633	.400
2	.7673	1.487	.935	.648	.409
3	1.6105	1.749	1.032	.692	.435
4	2.5700	2.106	1.191	.764	.474
5	3.5611	2.496	1.378	.852	.519
6	4.5592	2.893	1.574	.946	.563
7	5.5629	3.295	1.774	1.045	.607
8	6.4835	3.663	1.958	1.136	.646

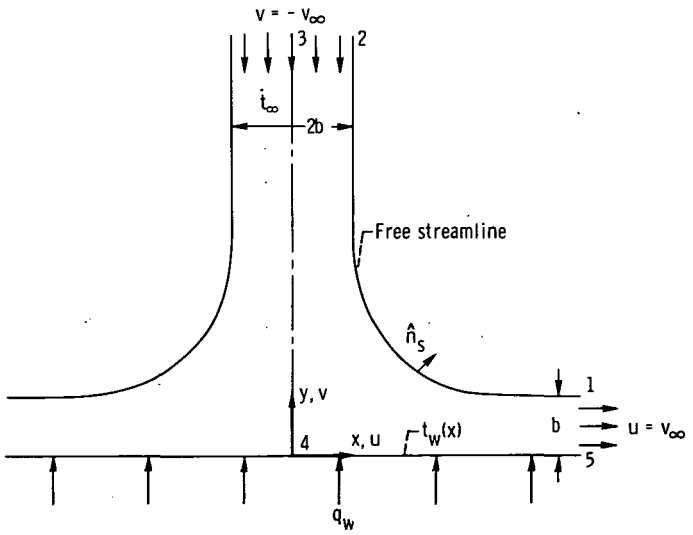

Figure 1. - Inviscid-irrotational jet impinging on plate with specified uniform heat addition.

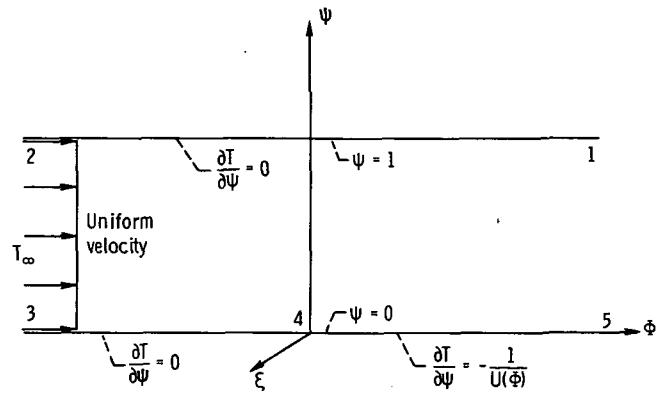

Figure 2. - Jet region mapped into potential plane.

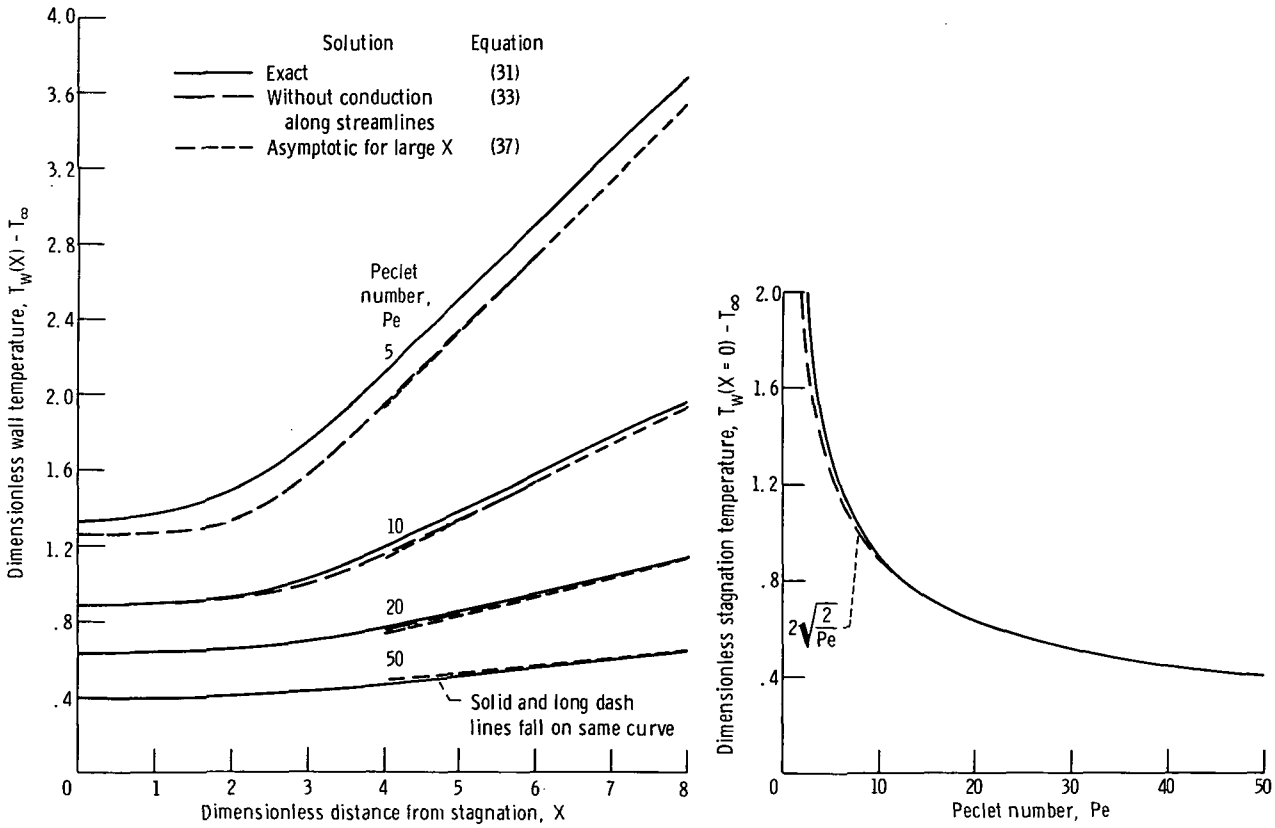

(a) Distribution along impingement plate.

(b) Dimensionless wall temperature at stagnation (X = 0); can be approximated with very small error for Pe > 10 by $T_w - T_\infty = 2\sqrt{2/Pe}$.

Figure 3. - Dimensionless wall temperature for impinging jet.

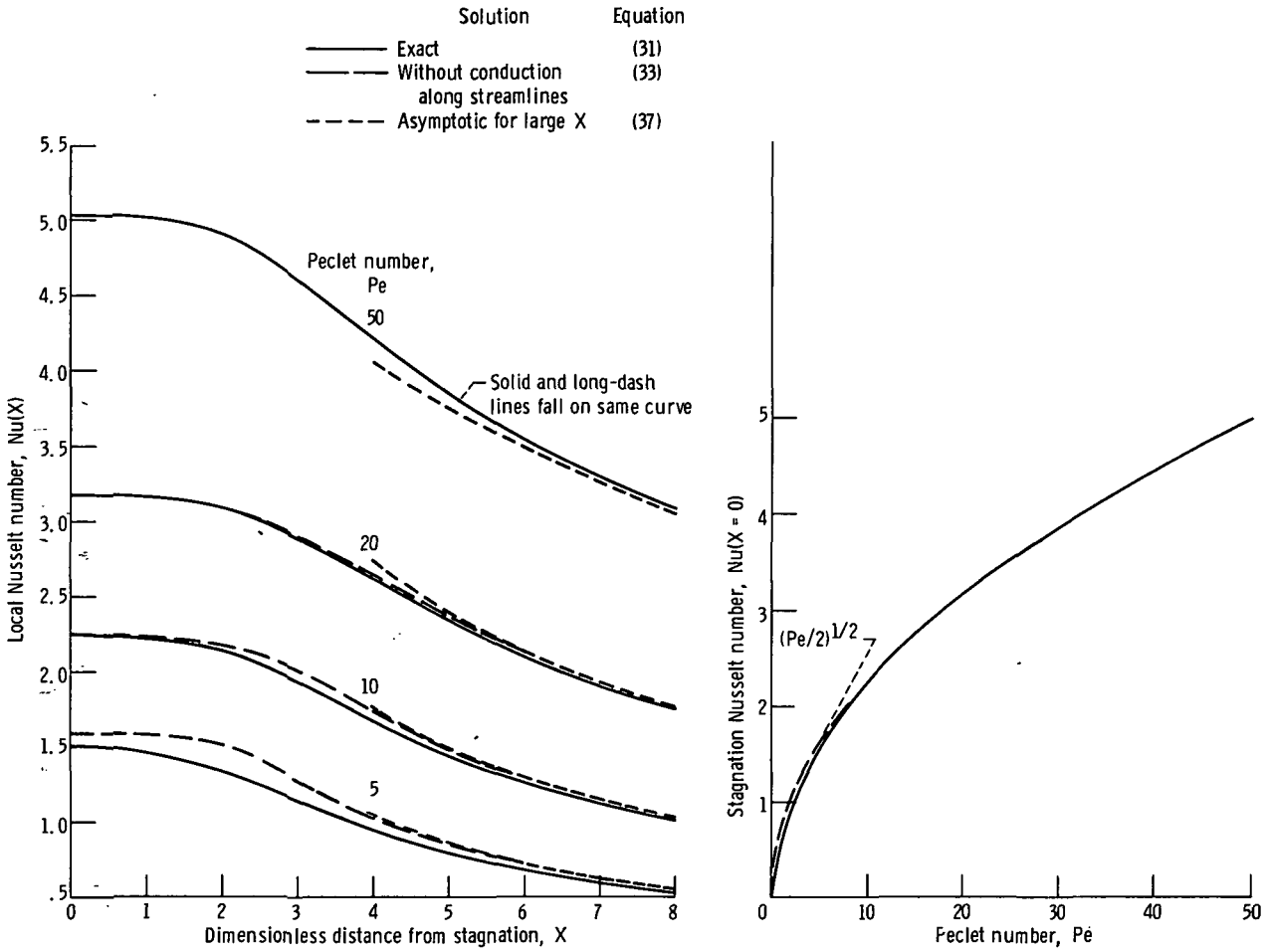

(a) Local Nusselt number along impingement plate.

(b) Nusselt number at stagnation (X = 0); can be approximated with very small error for Pe > 10 by Nu = $(Pe/2)^{1/2}$.

Figure 4. - Nusselt number for impinging jet.

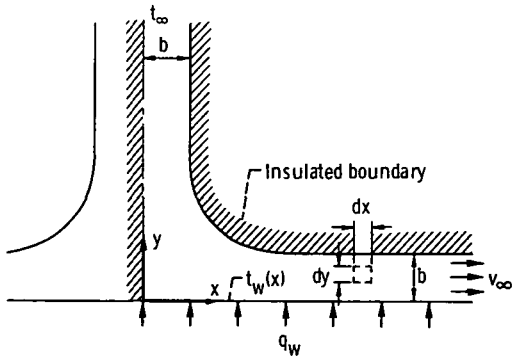

Figure 5. - Geometry for derivation of heat-transfer behavior at large x.

"The aeronautical and space activities of the United States shall be conducted so as to contribute . . . to the expansion of human knowledge of phenomena in the atmosphere and space. The Administration shall provide for the widest practicable and appropriate dissemination of information concerning its activities and the results thereof."

—NATIONAL AERONAUTICS AND SPACE ACT OF 1958

NASA SCIENTIFIC AND TECHNICAL PUBLICATIONS

TECHNICAL REPORTS: Scientific and technical information considered important, complete, and a lasting contribution to existing knowledge.

TECHNICAL NOTES: Information less broad in scope but nevertheless of importance as a contribution to existing knowledge.

TECHNICAL MEMORANDUMS: Information receiving limited distribution because of preliminary data, security classification, or other reasons. Also includes conference proceedings with either limited or unlimited distribution.

CONTRACTOR REPORTS: Scientific and technical information generated under a NASA contract or grant and considered an important contribution to existing knowledge.

TECHNICAL TRANSLATIONS: Information published in a foreign language considered to merit NASA distribution in English.

SPECIAL PUBLICATIONS: Information derived from or of value to NASA activities. Publications include final reports of major projects, monographs, data compilations, handbooks, sourcebooks, and special bibliographies.

TECHNOLOGY UTILIZATION PUBLICATIONS: Information on technology used by NASA that may be of particular interest in commercial and other non-aerospace applications. Publications include Tech Briefs, Technology Utilization Reports and Technology Surveys.

Details on the availability of these publications may be obtained from:

SCIENTIFIC AND TECHNICAL INFORMATION OFFICE

NATIONAL AERONAUTICS AND SPACE ADMINISTRATION

Washington, D.C. 20546